Research Journal of Applied Sciences, Engineering and Technology 10(12): 1384-1388, 2015
DOI: 10.19026/rjaset.10.1838
ISSN: 2040-7459; e-ISSN: 2040-7467

Submitted: March 25, 2015 Accepted: April 22, 2015 Published: August 25, 2015

Research Article

Effects of Temperature on Tunability of PbSe/PbSrSe Quantum Well Lasers in the Infrared Region

Majed Khodr
Department of Electronics and Communications Engineering, American University of Ras Al Khaimah, P.O. Box 10021, Ras Al Khaimah, United Arab Emirates

Abstract: Recently lead salts quantum well lasers which exhibit strong quantum optical effects, have been used to fabricate infrared diode lasers with wide single-mode tunability, low waste heat generation and large spectral coverage up to about 10 μm. Based on the energy dependent effective mass method, a theoretical model was developed to study the effects of band non parabolicty and temperature on the tunability of IV-VI PbSe/$Pb_{0.934}$ $Sr_{0.066}$ Se laser system. This study will show the effects of temperature as a function of well width on the emitted wavelength. Moreover, it will be shown that the effects of non parabolicity on the energy levels can't be ignored in the nano range well width.

Keywords: Breath analysis, infrared, lead salts, non-parabolicity, quantum well lasers

INTRODUCTION

Mid-IR Quantum Cascade Lasers (QCLs) are fabricated from large band gap GaAs and InP based III-V semiconductor structures designed to have inter subband transition energies that enable mid-IR photon emission. First developed at Bell Labs and now demonstrated by many other groups, QCLs have offered great hope as a new mid-IR light source for trace gas sensing. Since low energy subband separation is required for mid-IR light emission and the subband dispersions are parallel, such electron-phonon scattering will always be a detrimental upper laser state depopulation mechanism thus necessitating high electron currents to achieve population inversion.

A second cascade laser approach, pioneered by Yang *et al*. (2005) and replicated at the Naval Research Laboratory (Kim *et al*., 2007), involves use of narrow band gap GaSb based hetero-structures that employ a type II band alignment. In this case, lasing involves interband transitions between quantum confined conduction and valence subband states such that low energy mid-IR photons are generated. These lasers can benefit from the same cascade effect as QCLs, but since the lasing transitions are interband the subband dispersions for the relevant laser transition states are not parallel and this helps to reduce significantly upper laser transition state depopulation effects associated with electron-phonon scattering. Low Interband Cascade (IC) laser threshold currents provide strong evidence for the negative impact that electronphonon scattering can have on semiconductor lasers that utilize intersubband transitions. Interband mid-IR lasers, such as IC and IV-VI diode lasers, thus have inherent advantages over QCL-type intersubband mid-IR lasers.

The most established mid-IR laser technology involves interband transitions using traditional pn junction diode laser designs with narrow bandgap IV-VI semiconductors. First demonstrated in 1964 (Butler *et al*., 1964), IV-VI mid-IR lasers based on PbSe, PbSnSe and related alloys found early success in TDLS instrumentation and continue to be used today. Operating voltages are typically less than 300 mV and operation currents are typically in the 500 mA range, so power input levels are well below 1 watt, more than an order of magnitude better than QCLs. Currently, the main problem with IV-VI mid-IR lasers is the need for cryogenic cooling to obtain Continuous Wave (CW) emission. Also, there is a lack of studies on the effects of tunability temperatures on the device performance. Therefore, this study is necessary to understand and evaluate the device performance under several different temperature ranging from 77 to 300 k.

A theoretical model that is based on Kane's two band theory is being used to:

- Study the effects of band non parabolicity on energy level calculations and emitted wavelength.
- Determine the effects of temperature as a function of well width.

The key component of a laser spectrometer designed for sensitive chemical sensing is the tunable mid-IR laser with emission frequencies that match the fundamental rotational-vibrational frequencies of specific molecules. Although the first mid-IR lasers developed were based on the narrow band gap IV-VI

compound semiconductor family of materials (PbSe, PbTe, PbSnSe, PbSnTe, etc.), there has been and continues to be much attention focused on intersubband Quantum Cascade Laser (QCL) technology (Lehtinen and Kuusela, 2014; Razeghi *et al*., 2013). In the area of medical diagnostic applications, the amount of work demonstrated with IV-VI lasers far exceeds the amount of work demonstrated with QCLs. From a device physics point of view, interband lasers have the advantage of much lower threshold currents because, unlike intersubb and lasers, phonon scattering is not an effective mechanism for non-radiative interband transitions.

In the infrared region, lead salts IV-VI lasers may play a key role in breath analysis as a promising application and diagnostic tool that should perform well in clinical settings where real time breath analysis can be performed to assess patient health. Based on literature reports, health conditions such as Breast cancer and Lung Cancer have biomarker molecules in exhaled breath at wavelengths in the Infra-Red (IR) region (Buszewski *et al*., 2007; Zolotov, 2005; Roller *et al*., 2002). A new technique that may play a key role in detecting these biomarkers is Tunable Laser Spectroscopy (TLS) (Roller *et al*., 2002). Lead salts IV-VI tunable quantum well laser structures, as part of TLS system, can be used to generate these critical wavelengths that can be absorbed by the various biomarker molecules and hence detecting their presence in Parts per Million (PPM). Laser emission at these critical wavelengths is related to several system parameters (Roller *et al*., 2002; Shen *et al*., 2002) and hence a theoretical study that is based on device physics is needed to solve for the anisotropy in the constant energy surfaces and for the strong nonparabolicity of the bands of this type of material.

MATERIALS AND METHODS

Lead salts, such as *PbSe*, *PbSrSe* and *PbSeTe*, are direct energy gap semiconductors with band extrema at the four equivalent L points of the Brillouin zone. Because the conduction and valence bands at the L points are near mirror images of each other, the electron and hole effective masses are nearly equal. Furthermore, the bands are strongly non parabolic (Partin, 1988).

For a well material with parabolic bands in the growth direction (z-direction), the effective masses in the Schrodinger-like equation are at the extrema of the bands and they are independent of the energy. For a well material with non-parabolic bands in the z-direction, two methods can be used to solve for the energy levels.

The first method uses the "effective mass" equation, also known as the Luttinger-Kohn (LK) equation:

$$[E_z(k) + V_o]\chi = \varepsilon_n \chi \tag{1}$$

In the above equation E_z (k) is the energy dispersion in the unperturbed periodic lattice and, according to the Kane's model, the conduction-band energy can be expressed, up to order k^4, as:

$$E_z(k) = \frac{\hbar^2 k^2}{2m_w^*}\left(1 - \gamma k^2\right) \tag{2}$$

where m_w^* is the effective mass at the bottom of the conduction band and γ is a coefficient that depends on the system investigated. The energy levels are calculated by the same two equations derived for the parabolic bands, with the exception that the wave vector in the growth direction k takes the following form:

$$k^2 = (1/2\gamma)\left[1 - \sqrt{1 - 8\gamma E_z m_w^*/\hbar^2}\right] \tag{3}$$

This expression for k is found from Eq. (2). When $E_z(k)$ can be approximated as parabolic in k, Eq. (1) can be written in Schrodinger-like equation.

The second method is the "Energy-Dependent Effective Mass" (EDEM) method with m_w^*, is energy dependent according to the following equation:

$$m_w^*(E_z) = \frac{\hbar^2 k}{\partial E_z(k)/\partial k} \tag{4}$$

The band non-parabolicity effects can be considered by introducing this energy-dependent effective mass in the Schrodinger-like equation. This results in similar eigenvalue equations to those for parabolic bands with the exception that the effective mass of the well material is given by Eq. (4). Both methods can be used in the calculations of the energy levels for a non-parabolic band material.

The energy dispersion relation for lead salts in the z-direction, using Kane's model can be written as:

$$E_z = -\frac{1}{2}Eg \pm \sqrt{\frac{1}{4}Eg^2 + \frac{\hbar^2 Eg}{2m_w^*}k^2} \tag{5}$$

The dispersion relation for non-parabolic bands in the z-direction can be found by keeping higher order terms in the expansion, i.e., k^4 terms. The resultant dispersion relation for non-parabolic bands is given by:

$$E_z = \frac{\hbar^2 k^2}{2m_w^*}\left(1 - \frac{\hbar^2}{2m_w^* Eg}k^2\right) \tag{6}$$

for the valence and conduction bands. The zero energy is taken at the extrema of the corresponding band. To include the non-parabolicity effects on the parabolic energy levels, the energy-dependent effective mass approach requires the knowledge of $m_w^*(\varepsilon)$. Using

Eq. (4) and (5), the energy dependent effective mass is given by:

$$m_w^*(E_z) = m_w^*(1 + 2E_z/Eg) \quad (7)$$

On the other hand, the Luttinger-Kohn equation approach requires the knowledge of γ in Eq. (2) and (3). By comparing Eq. (2) with Eq. (6), the value of γ is found to be:

$$\gamma = \frac{\hbar^2}{2m_w^* Eg}$$

And hence:

$$k^2 = \left(m_w^* Eg/\hbar^2\right)\left[1 - \sqrt{1 - 4E_z/Eg}\right] \quad (8)$$

From this result one finds that the maximum energy level value that can be calculated is less than or equal to 1/4 Eg. The reason is the limitations imposed by the derivation of the Luttinger-Kohn Eq. (1) which was derived using the perturbation theory up to the second order (Hiroshima and Lang, 1986). However, this limitation can be overcome by establishing its validity up to the higher orders (Partin, 1988). Due to this limitation, the energy levels for the system under investigation were calculated using the EDEM method. On applying this model we made three assumptions:

- The difference in the energy gaps between the well material and the barrier material is assumed to be equally divided between the conduction and valence bands. This assumption is made because measurements on the offset energy for this system have not been made. In addition, experimental data on similar IV-VI material QW structures showed that the conduction and valence band offset energies are equal (Partin, 1988).
- The conduction and valence-band mobility effective masses in the well are assumed equal and the effective masses of the carriers outside the well are assumed constant. This assumption is made because it was shown that, for a first approximation, the effective mass is directly proportional to the energy gap and the conduction and valence-band mobility effective masses in the well were found almost equal (Partin, 1988).
- The effects of non-parabolicity of the barrier material are negligible. This assumption is made because the barrier thickness is large and the effects of non-parabolicity are very small for large thickness structures (Hiroshima and Lang, 1986).

The system of interest in this study is PbSe/$Pb_{0.934}Sr_{0.066}$ Sesingle quantum well where the barrier is $Pb_{0.934}Sr_{0.066}$ Se and the well is PbSe. The $Pb_{1-x}Sr_xSe$ system's energy gap and effective masses' dependence on temperature is according to these relations (Shen *et al*., 2002):

$$E_g(x,T) = 0.150 + 3.608x - 1.31x^2 + (0.430 - 3.09x + 6.495x^2) \times 10^{-3} T(eV)$$
(For $0 \le x \le 0.276$, $0 < T \le 350$ K) (9)

And the empirical equation for the effective mass in the growth direction:

$$m_{||}/m_o = 0.3013 \times E_g + 0.00407$$
(For $0.2 \le E_g \le 1.2$ *eV*) (10)

RESULTS AND DISCUSSION

From these two equations the energy gaps and effective masses for the well material and barrier material are calculated at five temperatures of interest to this study: 77, 200, 150, 250 and 300 K, respectively. These values were used in the model to calculate the conduction band and valence band energy levels and hence emitted wavelengths at each temperature.

Using the data and system parameters obtain from Eq. (9) and (10) at 300 K, the first four conduction energy levels were calculated and shown in Fig. 1. Similar results obtained for the valence band. The dashed lines represent the energy level calculations assuming parabolic band structures and the solid lines represent the energy levels calculations assuming non parabolic band structure. As shown in the figure, the energy levels including the effects of non parabolicity are lower than those excluding the effects of non-parabolicity and this difference is higher for small well width values and decreases as the well width is increased. Moreover, this effect is higher for higher quantized energy levels. As for the fourth energy level the model calculated the energy level including the effects of non parabolicity and it does not exist assuming parabolic bands. Therefore, for applications that require high energy levels it is important to include the effects of non parabolicity to be able to calculate all the energy levels.

Adding the calculated conduction energy levels, valence energy levels and well energy gap, the emitted wavelength values at 300 K for the system are calculated and shown in Fig. 2. Again, the effects of band non parabolicity on the calculations are included and compared to those for parabolic bands. From the above data, it is expected that the emitted wavelength values are higher including non-parabolicity and this difference is higher for smaller well widths and decreases as the well width increases. In what follows, the effects of non parabolicty are included in all figures and calculations of this system.

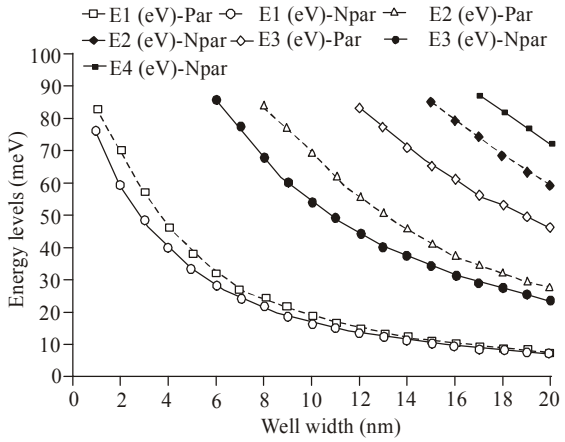

Fig. 1: The effects of non parabolicity on the conduction band energy levels at 300 K
Similar graph can be obtained for the valence band; the solid lines represent non-parabolic data; Dashed lines represent parabolic data

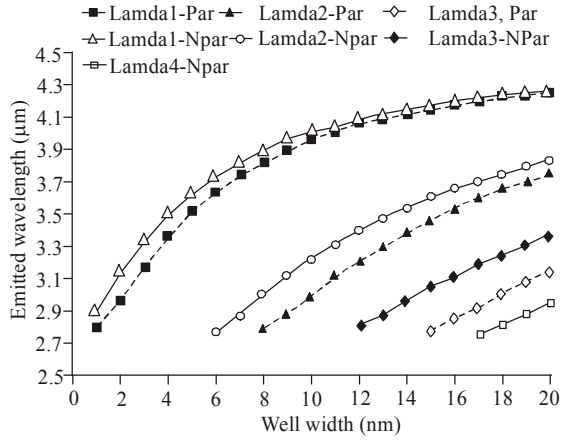

Fig. 2: The effects of non parabolicity on the emitted wavelengths at 300 K
The solid lines represent non-parabolic data; dashed lines represent parabolic data

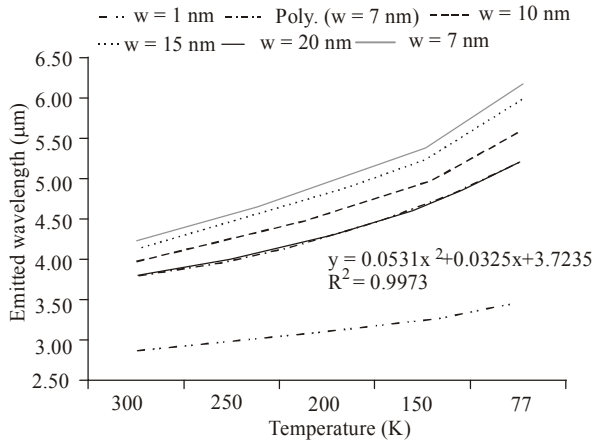

Fig. 3: The emitted wavelength widths
The polynomial equation is for the 7 nm well width

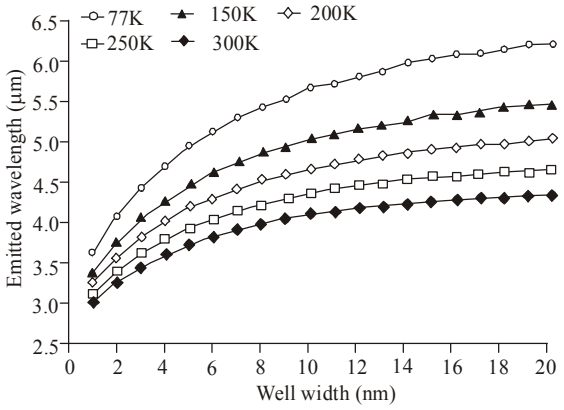

Fig. 4: First energy levels emitted wavelength as a function of well width with temperature as a parameter assuming non-parabolic data

From Eq. (9) and (10), we calculated the system parameters for the other four temperatures. The emitted wavelengths as a function of the five temperatures: 77, 150, 200, 250 and 300 K, respectively are shown in Fig. 3. As we decrease the temperature from 300 K at a fixed well width, the emitted wavelength increases. This means that the conduction band and valence band energy levels are shifting toward their corresponding band edge and hence reducing the effects of band non parabolicity on the emitted wavelength. Therefore, the emitted wavelengths calculations assuming parabolic band structures will not differ from those calculated assuming non parabolic band at lower operating temperatures.

The 7 nm well width is of particular interest to our laboratory work. As a result of best fitting the data, the emitted wavelength and temperature in Kelvin is given by the following polynomial relationship:

$$\lambda = 0.0531\,T^2 + 0.0325\,T + 3.7235 \qquad (11)$$

With the square of correlation factor $R^2 = 0.9973$. Similar relationships can be found for any well width thickness with slight differences to the polynomial constants. Figure 4 shows the emitted wavelength as a function of well width with temperature as a parameter. At a fixed temperature, increasing the well width will shift the energy levels to the band edge and hence the emitted wavelength will increase. From Fig. 3 and 4, one notices that the change in emitted wavelength is more noticeable between the 1 nm well width and the next higher well width (7 nm) for all temperatures. By increasing the well width, these changes between subsequent emitted wavelengths becomes smaller and smaller.

CONCLUSION

The intentions are to use this system as part of the Tunable Laser Spectroscopy system for detecting biomarkers in breath at specific and accurate

wavelengths (Roller *et al*., 2002; Yates, 2001; Owen *et al*., 1982; Smith *et al*., 2003). Examples include the measurement of exhaled nitric oxide for Asthma at 5.2 μm (Yates, 2001; Roller *et al*., 2002), Acetone for Diabetes at 3.4 μm (Owen *et al*., 1982), Acetaldehyde for Lung Cancer at 5.7 μm (Smith *et al*., 2003). Therefore, it is important to include the effects of non parabolicity to be able to obtain the desired accurate results for detecting the existence of volatile compounds at their corresponding wavelengths.

In this study, we analyzed $PbSe/Pb_{0.934}Sr_{0.066}SeSQW$ structure by calculating the first four quantized energy levels. The effects of band non parabolicity was studied and it was shown that non parabolicity will have small effect on quantized energy levels that are close to the band edge and it will have a larger effect on those far above the band edge. The tunability of the emitted wavelength as a function of temperature and data fitting showed a polynomial behavior for the well widths of interest. It was concluded that this single quantum well laser system is appropriate to use as part of Tunable Laser Spectroscopy technique.

REFERENCES

Buszewski, B., M. Kęsy, T. Ligor and A. Amann, 2007. Human exhaled air analytics: Biomarkers of diseases. Biomed. Chromatogr., 21: 553-566.

Butler, J.F., A.R. Calawa, R.J. Phelan Jr., T.C. Harman, A.J. Strauss and R.H. Rediker, 1964. PbTe diode laser. Appl. Phys. Lett., 5: 75-77.

Hiroshima, T. and R. Lang, 1986. Effects of conduction-band non-parabolicity onquantized energy levels of a quantum well. Appl. Phys. Lett., 49: 456-457.

Kim, C.S., C.L. Canedy, E.H. Aifer, M. Kim, W.W. Bewley *et al*., 2007. Molecular beam epitaxy growth of antimonide type-II "W" high-power interband cascade lasers and long-wavelength infrared photodiodes. J. Vac. Sci. Technol. B, 25: 991-994.

Lehtinen, J. and T. Kuusela, 2014. Broadly tunable quantum cascade laser in cantilever-enhanced photoacoustic infrared spectroscopy of solids. Appl. Phys. B, 115(3): 413-418.

Owen, E., V.E. Trapp, C.L. Skutches, M.A. Mozzoli, R.D. Hoeldtke, G. Boden and G.A. Reichard, 1982. Actetone metabolism during diabetic ketoacidosis. Diabetes, 31: 242-248.

Partin, L., 1988. Lead salt quantum effect structures. IEEE J. Quantum Elect., 24: 1716-1726.

Razeghi, M., N. Bandyopadhyay, Y. Bai, Q. Lu and S. Slivken, 2013. Recent advances in mid infrared (3-5μm) quantum cascade lasers. Opt. Mater. Express, 3: 1872-1884.

Roller, C.B., K. Namjou, J. Jeffers, M. Camp, P.J. McCann and J. Grego, 2002. Nitric oxide breath testing using tunable diode laser absorption spectroscopy: Application in respiratory inflammation monitoring. Appl. Optics, 41: 6018-6029.

Shen, W., H.F. Jiang, K. Wang, G. Yu, H.Z. Wu and P.J. McCann, 2002. Band gaps, effective masses and refractive indices of PbSrSe thin films: Key properties for mid-infrared optoelectronic devices applications. J. Appl. Phys., 91: 192-198.

Smith, D., T. Wang, J. Sule-Suso, P. Spanel and A.E. Haj, 2003. Quantification of acetaldehyde releases by lung cancer cells in vitro using selected ion flow tube mass spectrometry. Rapid Commun. Mass Sp., 17: 845-850.

Yang, R., C. Hill and B. Yang, 2005. High-temperature and low-threshold mid-infrared interband casade lasers. Appl. Phys. Lett., 87: 151109.

Yates, D.H., 2001. Role of nitric oxide in asthma. Immunol. Cell Biol., 79: 178-190.

Zolotov, Y.A., 2005. Breath analysis. J. Anal. Chem., 60: 497-497.